A 17,000-year glacio-eustatic sea level record: influence of glacial melting rates on the Younger Dryas event and deep-ocean circulation

Richard G. Fairbanks

Lamont-Doherty Geological Observatory of Columbia University, Palisades, New York 10964, USA

Coral reefs drilled offshore of Barbados provide the first continuous and detailed record of sea level change during the last deglaciation. The sea level was 121 ± 5 metres below present level during the last glacial maximum. The deglacial sea level rise was not monotonic; rather, it was marked by two intervals of rapid rise. Varying rates of melt-water discharge to the North Atlantic surface ocean dramatically affected North Atlantic deep-water production and oceanic oxygen isotope chemistry. A global oxygen isotope record for ocean water has been calculated from the Barbados sea level curve, allowing separation of the ice volume component common to all oxygen isotope records measured in deep-sea cores.

CHANGES in continental ice volume during the last deglaciation generally have been inferred from two indirect sources: (1) geological mapping of retreating ice margins, and (2) the marine oxygen isotope record. Direct estimates of glacial ice volume based on measured glacio-eustatic sea level changes are well documented from 9,000 years BP (before present)[1], but are poorly constrained before this time. Ruddiman[2,3] recently reviewed evidence supporting three different deglaciation models: (1) the 'smooth deglaciation' model with the most rapid change centred at 11,000 years BP; (2) the 'French two-step' deglaciation model with maximum melting rates from 14,000 to 12,000 years BP and from 10,000 to 7,000 years BP separated by a mid-deglacial pause with little or no ice volume loss; and (3) a 'younger Dryas' deglaciation model, which is distinguished from the French two-step model by a mid-deglacial reversal with significant ice growth from 11,000 to 10,000 years BP. Ruddiman concluded that the available evidence from marine and terrestrial records favoured the smooth deglaciation model. He further suggested that the stepwise decreases of $\delta^{18}O$ ($=([(^{18}O/^{16}O)_{sample}/(^{18}O/^{16}O)_{standard}]-1)\times 10^3$) apparent in many curves may not indicate sudden decreases in ice volume, but instead may be an artefact of a deep-ocean warming.

I sought to test the validity of these models, each with their own important climatic and oceanographic implications, by extending the existing coral-reef sea level curve[1] to the last glacial maximum. The fossil coral reefs surrounding Barbados are a very good system for examining the detail and timing of the last deglaciation. Here I show that the sea level curve derived from the Barbados reefs supports the French two-step model[4]. I then review the evidence for the oceanic and climatic response to this two-step deglaciation, with particular emphasis on understanding the cause of the Younger Dryas event.

Barbados corals

The Caribbean reef-crest coral *Acropora palmata* (Lamarck) is[1,5] the best available sea level indicator for Pleistocene studies. This species is generally restricted to the upper five metres of water and dominates the reef-crest community in many locations. *A. palmata* is one of the fastest growing corals and is often found in an interlocking reef framework on the windward side of Caribbean islands. Its massive size minimizes post-depositional transport and compaction, and its abundance and generally pristine aragonite skeleton make sampling for ^{14}C or $^{230}Th/^{234}U$ age dating relatively easy.

To reconstruct glacio-eustatic sea levels, I chose to core *A. palmata* on the south coast of Barbados for several reasons: (1) the offshore bathymetry is gently sloping compared with the precipitous drop surrounding many Caribbean volcanic islands or the Bahama Bank; (2) Barbados is rimmed by three parallel offshore ridges[6] for which I had extremely detailed bathymetric maps. Macintyre has suggested[6] that these ridges are associated with past sea level changes, comprising potentially thick sequences of *A. palmata*; (3) onshore exposure of the *A. palmata* facies deposited during the penultimate deglaciation[5] (isotope stage 6-5) indicates that the south coast of Barbados is being uplifted at ~34 cm kyr^{-1}. Field mapping of these onshore *A. palmata* deposits indicated that throughout the history of reef growth on Barbados, the most extensive areal and vertical distribution of *A. palmata* occurred on the south and south-east coast; (4) Barbados is located in the western tropical Atlantic where relative sea level is least affected by changes in the equipotential surface that are due to the changing gravitational attraction of the diminishing Northern Hemisphere ice sheet[7]. Possible drawbacks of selecting Barbados include: (1) the assumption that the late Quaternary mean uplift of Barbados is without significant episodic uplift or subsidence; (2) the dip-stick model of using oceanic islands to measure net ocean sea level changes may be too simple or may not apply to Barbados because it is situated on top of an accretionary prism between two oceanic plates. The only adequate way to test these geophysical assumptions is to perform the same drilling and dating experiment at other locations.

Barbados cores and their radiocarbon ages

Between 18 November and 6 December 1988, 16 cores were drilled from the RV *Ranger* offshore of the south coast of Barbados using a wire-line coring rig with a four-point mooring system. The purpose of this cruise was to core a continuous vertical sequence of *A. palmata* deposited during sea level rise associated with the last deglaciation. The stratigraphy of the ten longest cores and the corresponding ^{14}C ages are illustrated in Fig. 1. These results show that a nearly continuous sequence of *A. palmata* was recovered between 7,800 yr BP and 17,100 yr BP.

To help guide site selection three radiocarbon ages were determined while drilling was in progress. The remainder were

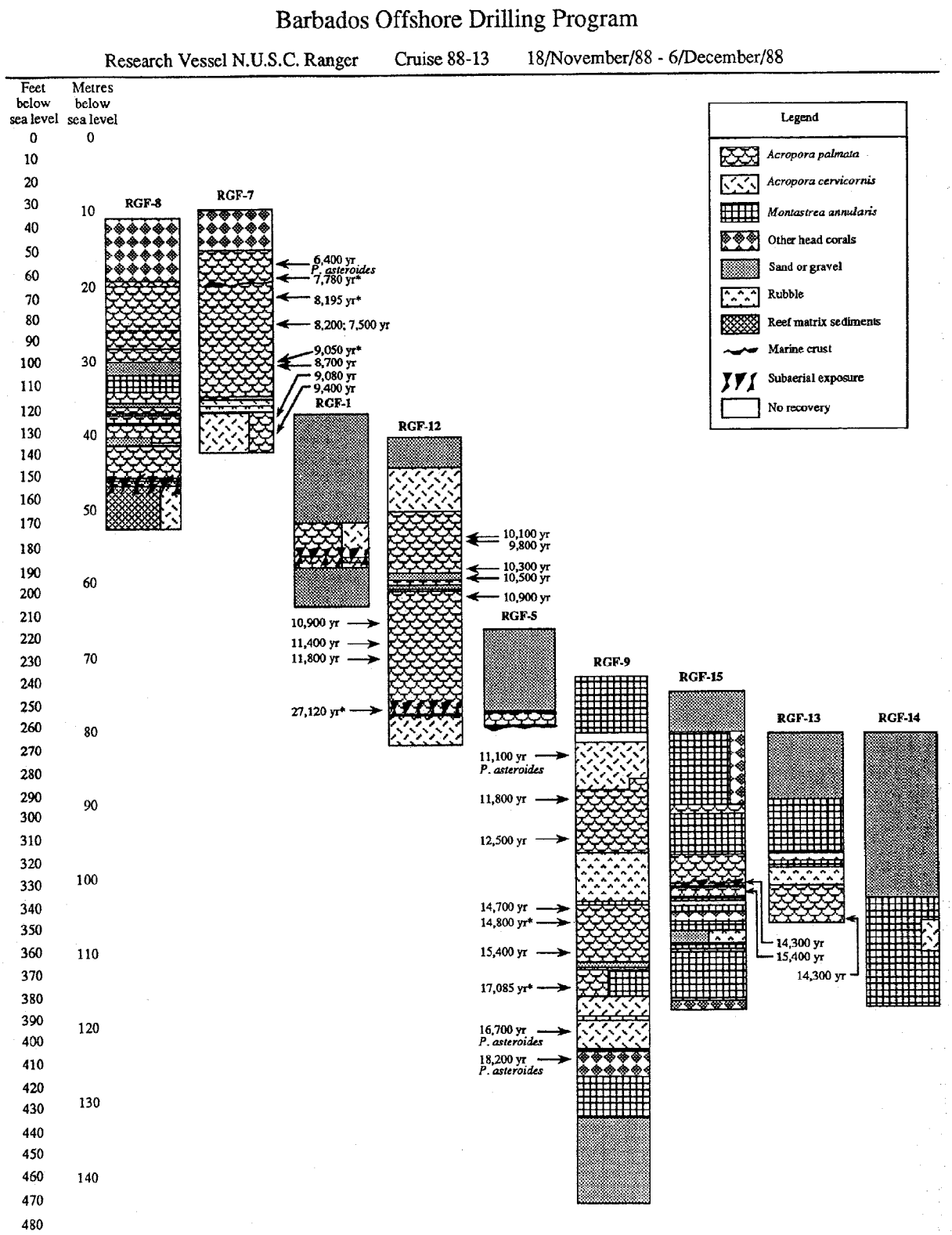

FIG. 1 Stratigraphic description of Barbados cores plotted against the modern sea level. Radiocarbon ages (yr) of individual corals are indicated by arrows. These ages are corrected for local seawater $\Delta^{14}C$ (the difference between the ^{14}C content of air and surface water) by subtracting 400 yr from the measured radiocarbon ages. All dated corals are *A. palmata* with four exceptions as noted where *P. asteroides* were dated. Sample at 25 m was dated twice and the 700-yr difference is assumed to arise from a ^{14}C laboratory error. The younger age is assumed to be incorrect because it is stratigraphically inconsistent with neighbouring samples. This value is therefore not included in Fig. 2. Ages marked by an asterisk were measured at Geochron Laboratory, all others at Lamont-Doherty. Samples below the subaerial exposure horizons in cores RGF-8 and RGF-1 have been dated at >44,000 radiocarbon years.

determined after the cruise using conventional liquid scintillation counting or gas proportional counting. The average analytical uncertainty (1σ) of these measurements is ±130 yr for ages less than 17,000 yr. All radicarbon ages are corrected for the apparent age of sea water at Barbados by subtracting 400 yr (ref. 8). Radiocarbon ages are not corrected for secular changes in the atmospheric ^{14}C which may be large during the deglaciation[9]. As part of a companion study, the $^{230}Th/^{234}U$ ages of these samples are being determined by mass spectrometry[10] to establish time-dependent changes in the surface ocean ^{14}C levels.

The deepest radiocarbon-dated sample of *A. palmata* occurs at 113.8 m below the present sea level (119.6 m if corrected for assumed mean uplift rate) and is dated to be 17,100 yr old. This age marks the end of the glacial period according to accelerator mass spectrometry (AMS) ^{14}C-dated $\delta^{18}O$ records from deep-sea cores[11,12]. A sample of *Porites asteroides* from 124 m below the present sea level is 18,200 yr old. This date provides a maximum sea level estimate of 131 m (uplift corrected) for the last glacial maximum. Unlike *A. palmata*, *P. asteroides* is not restricted to shallow depths so this glacial maximum sea level estimate must be taken as an extreme. Extrapolation of the sea level curve to 18,000 yr BP indicates a sea level of 121 ± 5 m below the present level during the last glacial maximum, the best estimate so far.

Between 17,100 and 12,500 yr BP, the sea level increased by 20 m (Fig. 2). This first phase of deglaciation was terminated by an exceedingly rapid sea level rise of 24 m in less than 1,000 radiocarbon years, termed melt-water pulse IA (mwp-IA). Melt-water pulse IA (12,000 yr BP) corresponds to the latter part of Termination Ia (14,500–11,500 yr BP) as defined in deep-sea $\delta^{18}O$ records (refs 4, 11, later modified in ref. 12). Melt-water pulse IA and Termination Ia overlap to some extent, but cannot be synonymous. The rate of sea level rise was at a minimum at 11,000 yr BP, marking the beginning of the Younger Dryas chronozone, and remained low until 10,500 yr BP. The last half of the Younger Dryas chronozone (10,500–10,000 yr BP) is marked by increasing rates of sea level change, culminating in melt-water pulse IB (mwp-IB) centred at 9,500 yr BP. During mwp-IB, which closely corresponds to Termination Ib in deep-sea terminology, the sea level rose ~28 m, similar to the sea level rise associated with mwp-IA.

Comparison of seasonal insolation changes

According to the Milankovitch theory[13] the Pleistocene ice ages were caused primarily by changes in the seasonal distribution of incoming radiation associated with orbit variations. The Northern Hemisphere ice sheets accumulate in the 40°–70° N latitude range whereas the Antarctic ice sheet is located poleward of 70° S. Insolation changes associated with the 41,000-yr tilt cycle increase poleward in both hemispheres, whereas the 23,000-yr precessional cycle dominates insolation changes at middle and low latitudes and is out of phase between hemispheres. Since the work of Milankovitch, the time-dependent patterns of radiation have been calculated more precisely[14]. The Barbados sea level provides the first direct and high-resolution comparison between the astronomical changes and continental ice response. In Fig. 3, the changes in insolation over the Laurentide/Fennoscandinavian ice sheet and the Antarctic ice sheet are compared with the melt-water discharge rates calculated from the Barbados sea level curve. The discharge rates are plotted in radiocarbon years and must be converted to calender years for comparison with the insolation curves[15]. Initial $^{230}Th/^{234}U$ dates by mass spectrometry indicate that the two melt-water pulses are not artefacts arising from distortions of the radiocarbon timescale (E. Bard, B. Hamelin and R.G.F., manuscript in preparation). The $^{230}Th/^{234}U$ age of mwp-IA is somewhat older, however, than the calibration curve[15] would indicate. Although the radiocarbon-age calibration is not well established beyond 9,000 yr BP (ref. 15), the absolute-age estimates for the two melt-water pulses are 13,070 and 10,445 calendar years BP based on the ^{14}C calibration of ref. 15. This comparison shows that the most intense interval of ice-sheet disintegration (13,070 calendar years BP) predates the Northern Hemisphere insolation maximum (centred at 11,000 years BP) by ~2,000 yr (Fig. 3). Melt-water pulse IB is 500 years younger than the insolation maximum. At present there is no astronomical explanation for separate melt-water pulses. The distribution of Northern Hemisphere ice and the retreat of its margins was not uniform[16], and the relative contribution and timing of Antarctic ice decay is not known. These as well as other factors, such as changing ocean and atmosphere circulation patterns, may explain the variable discharge rates.

The global oxygen isotope curve

The ^{14}C-dated Barbados sea level curve can be scaled to $\delta^{18}O$ using the calibration of 0.011‰ per metre change in sea level[5] (Fig. 2). This calibration is a maximum value and corresponds to a mean glacial-ice $\delta^{18}O$ value of −42‰ (standard mean ocean water). Based on ice-core $\delta^{18}O$ data from Greenland and Antarctica and modern $\delta^{18}O$ measurements in precipitation, this value provides a reasonable upper limit for mean ice composition for the entire deglaciation. The global $\delta^{18}O$ curve predicted from the Barbados sea level curve represents the ice volume component common to all $\delta^{18}O$ records from deep-sea cores. After taking into account the mixing time of the ocean, the global $\delta^{18}O$ curve can be subtracted from any high-resolution AMS ^{14}C-dated $\delta^{18}O$ curve to compare regional differences in the $\delta^{18}O$ of water and temperature.

Ocean $\delta^{18}O$ record of melt-water discharge rates

During mwp-IA and mwp-IB, glacial melt water discharged (primarily into the North Atlantic surface ocean) at maximum rates of 14,000 $km^3\ yr^{-1}$ and 9,500 $km^3\ yr^{-1}$ respectively (Fig. 3).

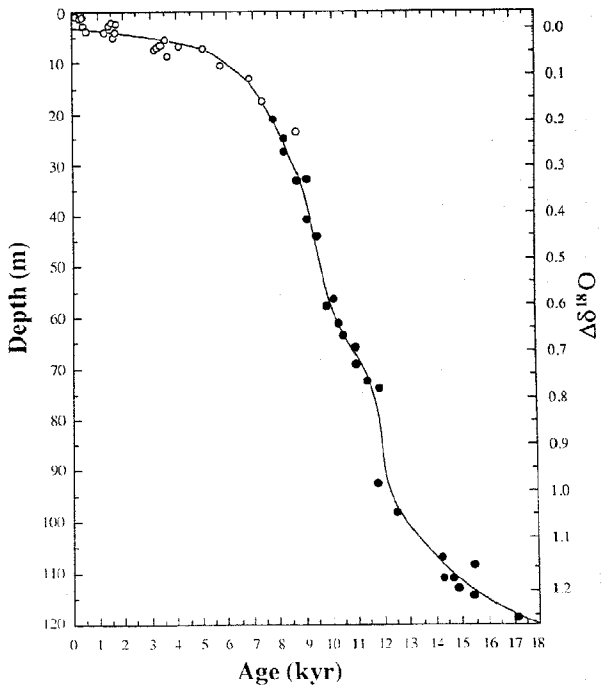

FIG. 2 Barbados sea level curve based on radiocarbon-dated *A. palmata* (filled circles) compared with *A. palmata* age-depth data[1] (open circles) for four other Caribbean island locations. All radiocarbon ages in this figure are corrected for local seawater $\Delta^{14}C$ by subtracting 400 yr from the measured radiocarbon ages[8] but they are not corrected for secular changes in atmospheric ^{14}C levels[15]. The Barbados data are corrected for the estimated mean uplift of 34 cm kyr^{-1}. The right-hand axis of the Barbados sea level curve (solid line) is scaled to the estimated $\delta^{18}O$ change of mean ocean water using the calibration in ref. 5.

These glacial-melt-water rates are comparable to the modern fresh-water discharge rate (11,400 $km^3\ yr^{-1}$) into the entire North Atlantic (0-90° N latitude)[17]. During the first half of the Younger Dryas chronozone between 11,000 and 10,500 yr BP, melt-water discharge averaged 2,700 $km^3\ yr^{-1}$, a factor of five less than discharge rates during mwp-IA and at least a factor of three less than rates during mwp-IB. By comparison, the modern discharge rates for the Mississippi and St Lawrence Rivers are 560 $km^3\ yr^{-1}$ and 330 $km^3\ yr^{-1}$ respectively[17].

The modern river discharge and marine precipitation is redistributed within the North Atlantic by ocean surface currents and results in strong oxygen isotope gradients of sea water in the north and north-west Atlantic bordering the subtropical gyre. Because glacial ice has very low $\delta^{18}O$ values relative to sea water, it is reasonable to assume that North Atlantic surface-water $\delta^{18}O$ distribution was dramatically affected by the sharp increase in seasonal melt-water discharge during mwp-IA and mwp-IB.

The oxygen isotopic composition of planktonic foraminifera is a function of both the ambient seawater oxygen isotopic composition and temperature. Foraminiferal species have different seasonal, geographic and vertical distributions whereas melt-water discharge is very seasonal. The most extensively dated (AMS ^{14}C) foraminiferal oxygen-isotope record in the North Atlantic is from piston core SU81-18 taken at a depth of 3,135 m near the coast of Portugal (37°46′ N, 10°11′ W)[12]. The oxygen isotope record of *G. bulloides* shows four distinct steps followed by $\delta^{18}O$ minima dated at 13,600, 12,300, 8,800 and 6,800 yr BP (Fig. 4). The two largest steps coincide with mwp-IA and mwp-IB. Although it is possible that these $\delta^{18}O$ shifts with minima at 12,300 and 8,800 yr BP are somehow related to local temperature changes, their coincidence with the salinity ($\delta^{18}O$) minima predicted by the Barbados sea level curve is strong evidence for regional salinity ($\delta^{18}O$) changes. I note that lower salinity and warmer temperatures both result in reduced $\delta^{18}O$ values of foraminiferal tests. Assuming an average glacial melt-water $\delta^{18}O$ value of −42‰, then the $\delta^{18}O$ of North Atlantic surface water will change at a corresponding rate of −1.2‰ for each 1‰ decrease in salinity. Therefore, the $\delta^{18}O$ minima in core SU81-18 (Fig. 4) can be produced by decreases in salinity of <1‰. The sea level increased only 10 m between 14,300 and 12,500 yr BP, an interval that spans the oldest $\delta^{18}O$ minima (13,600 yr) in core SU81-18.

Origin of the Younger Dryas event

In the preceding scenario, the Younger Dryas chronozone in the marine realm is characterized by minimal glacial-melt-water discharge, particularly between 11,000 and 10,500 yr BP, and is distinguished as an event primarily by its temporal position between two episodes of lower surface salinity. This interpretation of the origin of the Younger Dryas event is fundamentally different from the explanations involving the polar-front movements linked to ice-sheet elevation[2,3,12,18-20]. It is the exact opposite of explanations for the Younger Dryas that call upon maximum influxes of glacial ice and water between 11,000 and 10,000 yr BP[18-22].

Apparently there are very different regional responses to the melt-water pulses. For example, Mangerud *et al.*[23] have shown that in western Norway there were two major glacial re-advances into the North Sea at 12,200 and 10,000 yr BP. In the north-east Atlantic, unusually high abundances of the polar species *N. pachyderma sin* are found in association with the Vedde ash layer dated at 10,600 years BP (ref. 23). This peak abundance of polar species has been interpreted as a Younger Dryas cold event in the north-east Atlantic[18-20] although it apparently coincides with a low melt-water discharge rate. Ruddiman *et al.*[8] concluded that the Vedde ash, such as found at core site V23-81 on the Feni Drift, was delivered to the north-east Atlantic

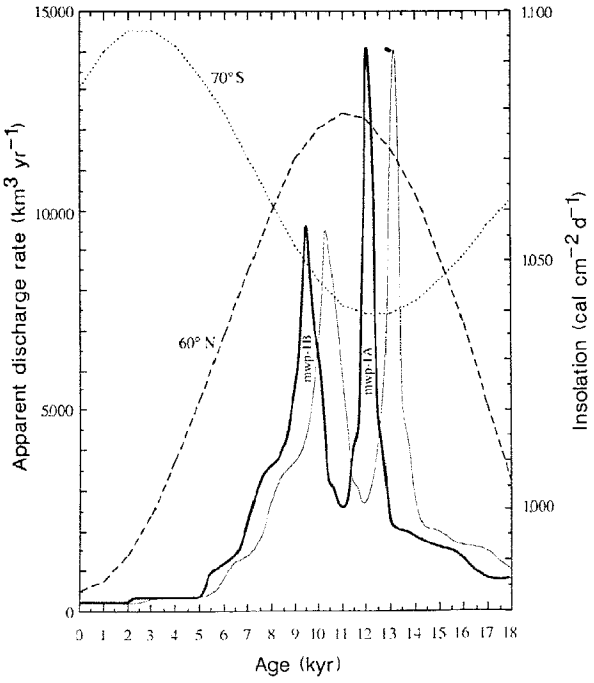

FIG. 3 The rate of glacial melt-water discharge calculated from the Barbados sea level curve compared to summer insolation. The discharge curve (thick line) is plotted according to radiocarbon years uncorrected for secular changes in atmospheric ^{14}C. Converting radiocarbon years BP to calendar years BP using the calibration in ref. 15 shifts the ages of mwp-IB and mwp-IA as shown by the thin line. Our preliminary $^{230}Th/^{234}U$ dates indicate that this correction is too small for mwp-IA (E. Bard, B. Hamelin and R.G.F., manuscript in preparation). By comparison, the insolation at 60° N (dashed line) and 70° S latitude (dotted line) are plotted against absolute time[14].

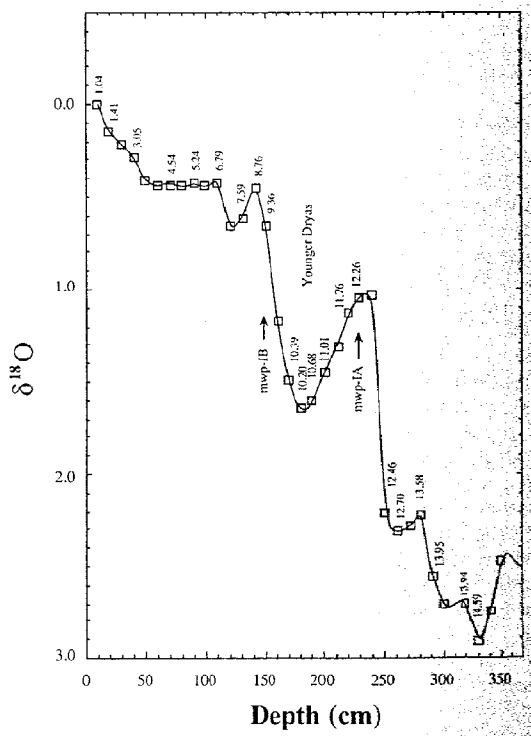

FIG. 4 The AMS ^{14}C-dated oxygen isotope record of *G. bulloides* from core SU81-18 located offshore of Portugal[12,34]. The AMS-^{14}C ages have been corrected for local seawater $\Delta^{14}C$ by subtracting 400 yr from the measured radiocarbon ages[8]. The estimated depth of mwp-IA and mwp-IB are marked by arrows.

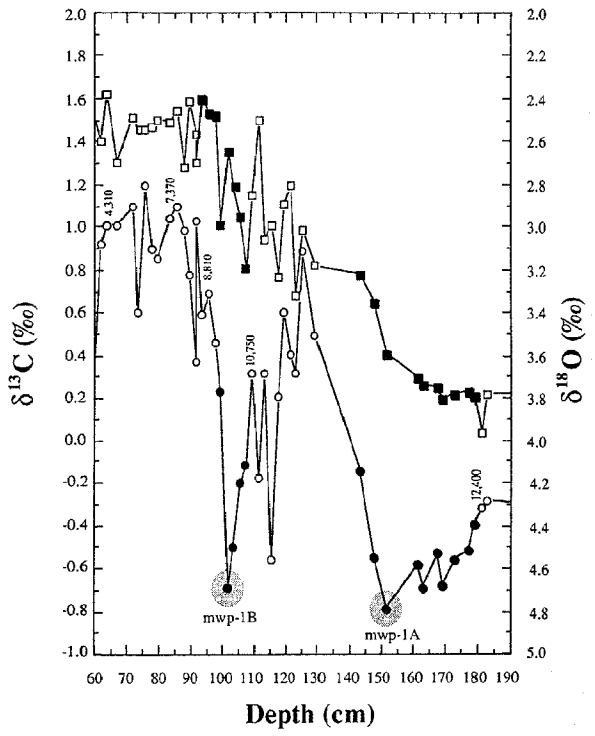

FIG. 5 Oxygen and carbon isotope data from core EN120GGC1[29] for the last deglacial interval. Age assignments are based on four AMS-^{14}C dates from a companion core that has been stratigraphically correlated to EN120GGC1[30]. Using this age model, δ^{13}C minima are approximately coincident with mwp-IA and mwp-IB. Closed symbols mark intervals around mwp-IA and mwp-IB and illustrate that δ^{13}C minima occur during the unidirectional shifts in δ^{18}O.

by sea ice originating in the Norwegian Sea. Recent sea-ice studies[24] show, however, that it is plausible that the *N. pachyderma sin* was also imported to the north-east Atlantic by entrapment in sea ice that had formed in the Norwegian Sea.

Lower surface-water salinities during mwp-IA and IB are not inconsistent with the faunal distributions in the north-east Atlantic described in, for example, ref. 18. Polar station PAPA, at 50° N latitude in the northeastern Pacific, has a low-salinity mixed layer and may be a good analogue for the North Atlantic at 12,000 and 9,500 yr BP. Today at station PAPA, an 8 °C seasonal warming of the thin mixed layer results in a seasonal succession of planktonic foraminiferal species from polar to subpolar assemblages[25]. Lower salinity might also help explain the evidence for warmer climates on the southern European continent during the Bølling-Allerød and Preboreal periods (see ref. 12 for a review). Lower surface salinities generally result in a thinner surface mixed layer with less thermal inertia. Energy-balance climate models show[26] that a thinner surface mixed layer in the North Atlantic (>40° N) leads to warmer surface temperatures over land in summer and fall. Much larger regional responses over Western Europe are predicted in three-dimensional global-climate-model simulations[26]. Conversely, the lack of melt-water stratification of North Atlantic surface waters during the Younger Dryas would allow a return to cooler deglacial conditions recorded by planktonic foraminifera in the North Atlantic ~10,600 yr BP (refs 19, 20, 27) and by western European continental vegetation.

Broecker *et al.*[27,28] dated the minimum δ^{18}O value (maximum melt-water discharge) in the Gulf of Mexico cores EN32-PC6 and EN32-PC4 at 11,840 and 12,000 yr BP, which are equivalent in age to the AMS ^{14}C-dated δ^{18}O minimum in North Atlantic core SU81-18 (12,260 yr BP)[12]. These two events correspond precisely with mwp-IA, dated at 12,000 yr BP (Fig. 3). Broecker *et al.*[27,28] noted that the maximum glacial-melt-water discharge from the Mississippi River was followed by minimal discharge between 10,500 (EN32-PC6) and 11,100 yr BP (EN32-PC4). They reasoned that this reduction in Mississippi discharge reflected a shift in the drainage from the Mississippi to the St Lawrence River and was not related to changes in glacial melting rates. They further speculated that the melt-water diversion caused a salinity decrease in the North Atlantic strong enough to result in a decrease in North Atlantic deep-water formation during the Younger Dryas. A reduction in the heat released from the ocean as the northward advection of subtropical surface waters ceased was associated with the reduced formation of North Atlantic deep water. The discharge curve derived from the Barbados sea level curve predicts a minimum in Mississippi discharge 11,000 yr BP and therefore it is unnecessary to call upon the unusual combination of events required by the model in refs 27, 28. Furthermore, the discharge curve may explain why no melt-water spike was ever identified in the North Atlantic oxygen isotope records corresponding to an assumed diversion of melt water during the Younger Dryas event.

Deep-water response to melt-water pulse

Broecker *et al.*[27,28] cite Cd/Ca and δ^{13}C data reported from Bermuda Rise core EN120GGC1[29] as evidence that melt water shut down the production of North Atlantic deep water during the Younger Dryas. Boyle and Keigwin's[29] age model for the deglacial section of core EN120GGC1 is based on linear interpolation between age assignments of 14,000 yr BP for Termination Ia and 8,500 yr BP for Termination Ib as well as correlation of the %$CaCO_3$ record with that of a neighbouring core that has two AMS ^{14}C dates on the deglaciation. These ages for Terminations Ia and Ib were taken from the AMS ^{14}C dates on North Atlantic core CH73-139C[11]. AMS ^{14}C studies on other cores have shown that core CH73-139C suffers from considerable bioturbation[12]. The revised ages for Termination Ia are 14,500–12,260 yr BP and for Termination Ib, 10,390–9,360 yr BP (ref. 12).

Applying a more accurate chronology to core EN120GGC1[30] shows that the two intervals of highest melt-water discharge are also characterized by extremely low δ^{13}C values, presumably because of reduced influence of North Atlantic deep water at this site (Fig. 5). The section corresponding to Younger Dryas interval begins with high δ^{13}C values which then decrease to a minimum value during Termination 1b. If this revised timescale

Cloning by functional expression of a member of the glutamate receptor family

Michael Hollmann, Anne O'Shea-Greenfield, Scott W. Rogers & Stephen Heinemann

Molecular Neurobiology Laboratory, The Salk Institute for Biological Studies, La Jolla, California 92037, USA

We have isolated a complementary DNA clone by screening a rat brain cDNA library for expression of kainate-gated ion channels in Xenopus oocytes. The cDNA encodes a single protein of relative molecular mass (M_r) 99,800 which on expression in oocytes forms a functional ion channel possessing the electrophysiological and pharmacological properties of the kainate subtype of the glutamate receptor family in the mammalian central nervous system.

THE synapse plays a key role in the nervous system, and it is likely that biochemical changes at the synapse underlie some aspects of higher brain function. Most plausible theories of learning, for example, depend upon changes in the efficiency of chemical synapses[1,2]. Glutamate receptors are believed to play a central part both in memory aquisition and the establishment of "topographical maps"[3,4]. Hence, this receptor family has become the focus of much experimental work. Glutamate receptors are found throughout the mammalian brain and represent the predominant excitatory neurotransmitter system[3]. The best-studied glutamate receptors are ligand-gated ion channels that are permeable to cations. Based on pharmacological and electrophysiological data these receptors have been classified into four main subtypes: NMDA (*N*-methyl-D-aspartate), quisqualate, kainate and 2-amino-4-phosphonobutyrate[5] (APB). Recently, a G protein-coupled glutamate receptor representing a fifth class with a very different mechanism of action has been identified[6]. The fact that the subtypes show differences in their distribution in the brain[7] indicates that they represent distinct gene products with unique structures and functions.

Despite the prominent part these receptors play in normal synaptic transmission as well as in neuronal plasticity, their molecular characteristics have remained elusive, mainly because of a lack of ligands that bind irreversibly and with high specificity. Conventional biochemical approaches to the isolation of these receptors have so far either not succeeded in progressing beyond crude receptor solubilization, as is the case for the NMDA[8] and quisqualate[9] subtypes, or have resulted in the isolation of ligand-binding proteins for kainate[10–12] or glutamate[13,14] whose functions remain unclear. To circumvent these problems, we adopted a different approach involving the use of an oocyte expression system[15] to guide the selective cloning of cDNAs encoding functional glutamate-gated ion channels.

Here, we report the isolation of a cDNA clone, GluR-K1, from a rat forebrain cDNA library. This clone, on transcription *in vitro* and injection into *Xenopus* oocytes, expresses a functional glutamate receptor with the pharmacological properties of the kainate subtype. The primary structure of the protein encoded by the GluR-K1 cDNA has been deduced, and it is compared with the sequences of other ligand-gated ion channels, the nicotinic acetylcholine receptors (nAChR), and the glycine and γ-aminobutyric acid ($GABA_A$) receptors. The pattern of distribution of GluR-K1 mRNA is described and compared with kainate binding sites in the brain.

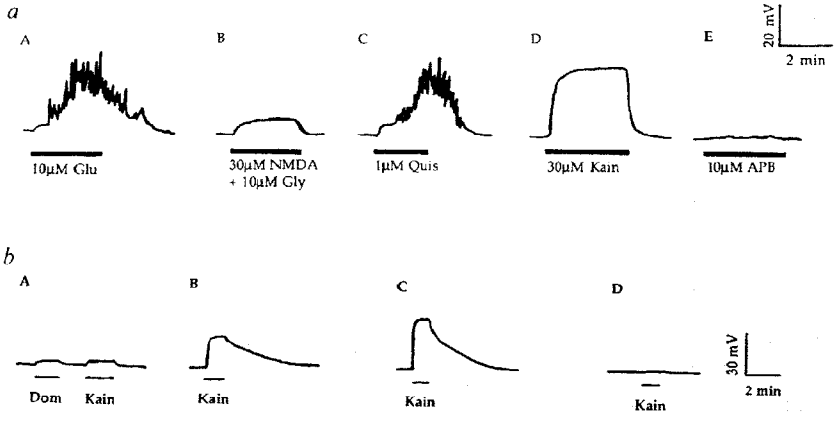

FIG. 1 *a*, Voltage traces obtained from a single *Xenopus* oocyte injected with 75 ng poly(A)$^+$ RNA isolated from rat forebrain 2 days before recording. Bars indicate duration of superfusion with indicated agonists. Glu, L-glutamate; NMDA, *N*-methyl-D-aspartate; Gly, glycine; Quis, quisqualate; Kain, kainate; APB, 2-amino-4-phosphonobutyrate. *b*, Voltage recordings from *Xenopus* oocytes 10 days (trace A) or 3 days (traces B–D) after injection with 25 ng λZAP RTB1 sense *in vitro* RNA (total library of 850,000 independent clones) (A), 25 ng λZAP-GluR-K1 sense *in vitro* RNA(B), 1.25 ng of pGluR-K1 sense *in vitro* RNA(C) or 1.25 ng of pGluR-K1 antisense *in vitro* RNA(D). Dom, domoate (10 μM); Kain, kainate (100 μM). Bars indicate duration of superfusion with agonist. METHODS. RNA was isolated from rat total forebrain by the guanidine isothiocyanate method[39] and subsequently poly(A)$^+$ selected[40]. The Uni-Zap™ XR cloning kit from Stratagene was used to construct a directional cDNA library of 850,000 independent clones in the bacteriophage expression vector λZAP II, where the insert clones are flanked by T3 and T7 RNA polymerase promoters at their 5′ and 3′ ends, respectively, allowing sense as well as antisense transcription[41]. DNA from pools of phage clones was linearized with Xho I, and diguanosine triphosphate-capped RNA was synthesized *in vitro* using the RNA transcription kit from Stratagene. A DNAse I digest was performed to remove the template after synthesis. *Xenopus* oocytes were prepared as previously described[33] and injected with 1–100 ng RNA, usually in a volume of 50 nl. Injected oocytes (20 per batch of RNA to be tested) were maintained in daily changed Barth's saline[33] at 17 °C. During the initial stages of the library screening, oocytes were checked for responses after 3, 5, 7, 9 and 10 days. During later stages of the screening, recordings were made on days 3 and 5 after injection. To facilitate rapid, sensitive screening of large numbers of oocytes we used voltage recording rather than voltage clamp, as described previously[33]. Depolarizations as small as 1–2 mV could be measured reliably.

for core EN120GGC1 is accurate, then the Younger Dryas and Preboreal chronozones are so condensed that bioturbation must be considered as a significant influence. The fact that a relatively subtle adjustment of age assignments can alter the interpretation of deep ocean response to deglaciation emphasizes the necessity for AMS ^{14}C dating of splits of the same samples used for stable isotope and Cd/Ca measurements in core EN120GGC1. Until this is done, it is equally plausible to suggest that the production of North Atlantic deep water was reduced or shut down within the Bølling/Older Dryas (mwp-IA) and Preboreal (mwp-IB) chronozones and not during the Younger Dryas.

Continental record of melt-water discharge rates

The rapid disintegration of the Northern Hemisphere ice sheets during mwp-IA and mwp-IB must have introduced large volumes of low-$\delta^{18}O$ melt water into the North Atlantic during the summer season. This $\delta^{18}O$-spiked melt water has two possible fates: entrainment in North Atlantic deep water or evaporation[17]. Because deep-water formation may have been halted briefly during the peak discharge, evaporation of $\delta^{18}O$-spiked surface water must have occurred to some extent.

The Greenland ice cores Dye 3[31-33] and Camp Century are both marked by two distinct $\delta^{18}O$ minima during deglaciation (Fig. 6). Many researchers assumed that these $\delta^{18}O$ minima indicated cooler temperatures[29-32] and that they were associated with a southward migration of the North Atlantic polar front[19,20]. However, recent ^{14}C dating of air bubbles in the Dye 3 ice core[33] enables a direct comparison to the ^{14}C dated Barbados sea level curve (Fig. 6). Six AMS ^{14}C measurements were made on samples taken at depths between 1,660 and 1,780 m (ref. 33). Using the age-depth relationship (squared correlation coefficient = 0.93) determined from these data, the estimated age for the $\delta^{18}O$ minimum at 1,792 m (Fig. 6) is 9,320 ^{14}C-years BP. The age of this $\delta^{18}O$ minimum in Dye 3 matches the age for mwp-IB (9,500 ^{14}C-years BP). It is not clear whether the ^{14}C age is concordant with the estimated calendar age based upon annual layer counts[31], because the radiocarbon timescale is not well calibrated in this time range. I believe that these presumed temperature minima in the Greenland $\delta^{18}O$ records may in fact be the result of source-water variability as well as temperature. If so, they may be the terrestrial equivalents of $\delta^{18}O$ minima in deep-sea cores such as SU81-18 (Fig. 4).

The immediate implications of the Barbados sea level record compel us to re-evaluate some of the traditional depictions of the Younger Dryas event. Whether or not the reinterpretations presented here are correct depends on the reliability of correlations between radiocarbon-dated marine and terrestrial signals. My results emphasize the primary role of melt-water discharge rates on the production of North Atlantic deep water and rapid climate change in western Europe. □

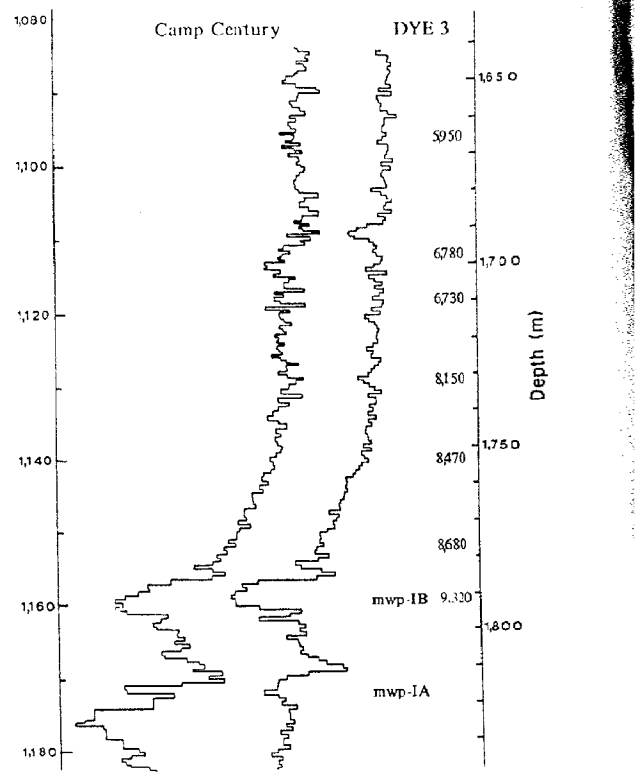

FIG. 6 Plot of terrestrial $\delta^{18}O$ records from Greenland ice cores Dye 3 and Camp Century[31,32] with six radiocarbon ages[33] indicated for Dye 3. Age for mwp-IB is estimated from the ^{14}C–depth relationship[33].

Received 18 May; accepted 19 October 1989.

1. Lighty, R. G., Macintyre, I. G. & Stuckenrath, R. *Coral Reefs* **1,** 125–130 (1982).
2. Ruddiman, W. F. in *North American and Adjacent Oceans During the Last Deglaciation* (eds Ruddiman, W. F. & Wright, H. E. Jr) **K-3** 463–478 (Geol. Soc. Am., Boulder, 1987).
3. Ruddiman, W. F. in *North American and Adjacent Oceans During the Last Deglaciation* (eds Ruddiman, W. F. & Wright, H. E. Jr) **K-3** 137–154 (Geol. Soc. Am., Boulder, 1987).
4. Duplessy, J. C., Delibrias, G., Turon, J. L., Pujol, C. & Duprat, J. *Palaeogeogr. Palaeoclimatol. Palaeoecol.* **35,** 121–144 (1981).
5. Fairbanks, R. G. & Matthews, R. K. *Quat. Res.* **10,** 181–196 (1978).
6. Macintyre, I. G. *Am. Ass. Petrol. Geol. Bull.* **56,** 720–738 (1972).
7. Clark, J. A., Farrell, W. E. & Peltier, W. R. *Quat. Res.* **9,** 265–287 (1978).
8. Bard, E. *Palaeoceanography* **3,** 635–645 (1988).
9. Oeschger, H. *et al. Radiocarbon* **22,** 299–310 (1980).
10. Edwards, R. L., Chen, J. H., Ku T.-L. & Wasserburg, G. L. *Science* **236,** 1547–1553 (1987).
11. Duplessy, J.-C. *et al. Nature* **320,** 350–352 (1986).
12. Bard, E. *et al. Nature* **328,** 791–794 (1987).
13. Milankovitch, M. M. *Canon of Insolation and The Ice-Age problem* (Koniglich Serbische Akademie, Beograd, 1941). English translation published by the U.S. Department of Commerce and the NSF, Washington, DC.
14. Berger, A. L. *Quat. Res.* **35,** 215–240 (1978).
15. Stuiver, M. *et al. Radiocarbon* **28,** 969–979 (1986).
16. Andrews, J. T. in *North American and Adjacent Oceans During the Last Deglaciation* (eds Ruddiman, W. F. & Wright, H. E. Jr) **K-3** 13–38 (Geol. Soc. Am., Boulder, 1987).
17. Baumgartner, A. & Reichel, E. *The World Water Balance* (Elsevier, New York, 1975).
18. Ruddiman, W. F., Sancetta, C. D. & McIntyre, A. *Phil. Trans. R. Soc.* **B280,** 119–142 (1977).
19. Ruddiman, W. F. & McIntyre, A. *Science* **212,** 617–627 (1981).
20. Ruddiman, W. F. & McIntyre, A. *Palaeogeogr. Palaeoclimatol. Palaeoecol* **35,** 145–214 (1981).
21. Mercer, J. H. *Arctic Alpine Res.* **1,** 227–234 (1969).
22. Johnson, R. G. & McClure, B. T. *Quat. Res.* **6,** 325–353 (1976).
23. Mangerud, J., Lie, S. E., Furnes, H., Kristiansen, I. L. & Lomo, L. *Quat. Res.* **21,** 85–104 (1984).
24. Spindler, M. & Dieckmann, G. S. *Polar Biol.* **5,** 185–191 (1986).
25. Reynolds, L. & Thunell, R. C. *J. Foraminiferal Res.* **15,** 282–301 (1985).
26. Schneider, S. H., Peteet, D. M. & North, G. R. in *Abrupt Climate Change* (eds Berger, W. H. & Labeyrie, L. D.) 399–418 (Reidel, Dordrecht, 1987).
27. Broecker, W. S. *et al. Palaeoceanography* **3,** 1–19 (1988).
28. Broecker, W. S. *et al. Nature* **341,** 318–321 (1989).
29. Boyle E. A. & Keigwin, L. *Nature* **330,** 35–40 (1987).
30. Keigwin, L. D., Jones, G. A. *Deep Sea Res.* **36,** 845–867 (1989).
31. Hammer, C. U., Clausen, H. B. & Tauber, H. *Radiocarbon* **28,** 284–291 (1986).
32. Dansgaard, W., White, J. W. & Johnson, S. J. *Nature* **339,** 532–534 (1989).
33. Andree, M. *et al. Radiocarbon* **28,** 417–423 (1986).
34. Bard, E. *Quat. Res.* **31,** 381–391 (1989).

ACKNOWLEDGEMENTS. For help with various aspects of the cruise and technical assistance I thank W. Svendsen (Longyear Co.), P. Gemeinhardt, K. Taylor and his drilling crew (Fugro McClelland Inc.), Captain M. Bordeaux, Firstmate P. Scott and the crew of the RV *Ranger*, R. Miller, T. Baker, C. Charles, T. Janacek, R. Lighty, D. Oppo, C. Ravelo, L. Barker, W. Hunte, P. McConney and Mr. Hope. I also thank G. Mathieu for the ^{14}C age determinations, E. Bard, W. Broecker, G. Kukla, E. Lighty, R. Peltier, W. Ruddiman and J. Wright for discussions, L. Keigwin and J. C. Duplessy for reviews and R. Matthews for his continued cooperation and advice on the Pleistocene history of Barbados. This research was supported by the NSF.